https://doi.org/10.1038/s41586-019-1110-x

Resonant electro–optic frequency comb

Alfredo Rueda[1,2,3,4,5,6], Florian Sedlmeir[1,2], Madhuri Kumari[5,6], Gerd Leuchs[1,2,5,6,7] & Harald G. L. Schwefel[5,6]*

[1]Max Planck Institute for the Science of Light, Erlangen, Germany. [2]Institute for Optics, Information and Photonics, University Erlangen-Nuernberg, Erlangen, Germany. [3]School in Advanced Optical Technologies (SAOT), Erlangen, Germany. [4]Institute of Science and Technology Austria, Klosterneuburg, Austria. [5]The Dodd-Walls Centre for Photonic and Quantum Technologies, Dunedin, New Zealand. [6]Department of Physics, University of Otago, Dunedin, New Zealand. [7]Institute of Applied Physics, Russian Academy of Sciences, Nizhny Novgorod, Russia.
*e-mail: harald.schwefel@otago.ac.nz

Supplement: Resonant Electro-Optic Frequency Comb

Alfredo Rueda
Max Planck Institute for the Science of Light, Staudtstr. 2, 90158 Erlangen, Germany
Institute for Optics, Information and Photonics,
University Erlangen-Nuernberg, Staudtstr. 7/B2, 91058 Erlangen, Germany
SAOT, School in Advanced Optical Technologies, Paul-Gordan-Str. 6, 91052 Erlangen, Germany
Institute of Science and Technology Austria, am Campus 1, 3600 Klosterneuburg, Austria
The Dodd-Walls Centre for Photonic and Quantum Technologies, New Zealand and
Department of Physics, University of Otago, Dunedin, New Zealand

Florian Sedlmeir
Max Planck Institute for the Science of Light, Staudtstr. 2, 90158 Erlangen, Germany and
Institute for Optics, Information and Photonics,
University Erlangen-Nuernberg, Staudtstr. 7/B2, 91058 Erlangen, Germany

Gerd Leuchs
Max Planck Institute for the Science of Light, Staudtstr. 2, 90158 Erlangen, Germany
Institute for Optics, Information and Photonics,
University Erlangen-Nuernberg, Staudtstr. 7/B2, 91058 Erlangen, Germany
Institute of Applied Physics, Russian Academy of Sciences,
46 UL'yanov Street, 603950, Nizhny Novgorod, Russia
The Dodd-Walls Centre for Photonic and Quantum Technologies, New Zealand and
Department of Physics, University of Otago, Dunedin, New Zealand

Madhuri Kumari and Harald G. L. Schwefel*
The Dodd-Walls Centre for Photonic and Quantum Technologies, New Zealand and
Department of Physics, University of Otago, Dunedin, New Zealand
(Dated: February 13, 2019)

CONTENTS

I. SUPPLEMENTARY MATERIAL

The structure of this supplementary material is as follows. First we describe optical whispering gallery mode (WGM) resonators and discuss the modal distribution. Then we introduce the mathematical formalism to describe a second order nonlinear interaction in the Hamiltonian description and consider the phase matching. We derive and solve the suitable rate equations in the Heisenberg picture. Finally we compare the efficiency of the process to the π-Voltage and discuss the experimental microwave coupling.

* harald.schwefel@otago.ac.nz

A. Optical Whispering Gallery Modes & Dispersion

A whispering gallery mode resonator usually consists of a convex shaped dielectric material with refractive index n higher than its surrounding [1]. At an angle beyond the critical angle the light undergoes total internal reflection and is guided on a circular path along the rim without refractive loss. Light can be coupled into the WGM through an evanescent field coupler such as a prism. In a physical resonator loss is always present and we distinguish between intrinsic loss rate γ' and coupling loss rate γ due to the interaction of the prism. If the resonator is critically coupled the coupling loss equals the intrinsic loss $\gamma' = \gamma$ and the photon number in the resonator is maximized. The total loss rate is $\Gamma = \gamma + \gamma'$. In a prism coupled WGM system we have control over the coupling rate γ by adjusting the distance of the prism from the resonator. Through careful adjustment, we can over-couple ($\gamma > \gamma'$) and under-couple ($\gamma < \gamma'$) the resonator. The total loss rate is related to the photon lifetime in the resonator as $\tau_p = 1/2\Gamma$ considering that the rates are defined for the field. The quality factor is $Q = \omega\tau_p$, where ω is the frequency of the resonance. The free spectral range corresponds to the inverse of the roundtrip time

$$\mathrm{FSR} = 1/\tau = c/(2\pi nR), \tag{1}$$

where R and c are the radius and the speed of light, respectively.

In a linear resonator the resonant frequency simply follows from the argument that an integer number of wavelengths needs to fit into the optical path length $\lambda_0 = 2\pi nR/m$ or equivalently $\omega = 2\pi \cdot m \cdot \mathrm{FSR}$ and $nk_0 = m/R$, with the wavenumber in free space $k_0 = \omega/c$. For very large WGM resonators this might still be a valid expression. It does not however take the actual geometric dispersion seen in a three dimensional WGM into account. In order to find better expressions for WGM resonators we need to consider the Helmholtz equation, with the appropriate boundary conditions given by the geometry. Here we choose a local toroidal coordinates system following Ref. [2, 3]. In such coordinates the scalar field inside of the resonator and outside of the resonator can be written as:

$$\mathbf{E}^{\eta}_{q,p,m}(\mathbf{r}(\rho,\varphi,\theta)) \approx \begin{cases} E_0 \exp(-\frac{\theta^2}{2\theta_m^2}) H_p(\frac{\theta}{\theta_m}) \mathrm{Ai}[f^{\eta}_{m,q}(\rho)] e^{im\varphi} & \text{if } \rho < \rho' \\ E'_\eta \exp(-\frac{\theta^2}{2\theta_m^2}) H_p(\frac{\theta}{\theta_m}) \exp(-\kappa(\rho-\rho')) e^{im\varphi} & \text{if } \rho > \rho', \end{cases} \tag{2}$$

where $r(\rho,\varphi,\theta)$ is the position relative to the toroidal coordinates origin ρ and θ stand for the distance and polar angle relative to the center of the curvature of the rim and ρ' is the lateral radius of the WGM resonator. η is the polarization index parallel (TE) and orthogonal (TM) to the symmetry axis, $\kappa_\eta = k_0\sqrt{n_\eta^2 - 1}$ the evanescent decay constant. $q = \{1, 2 \ldots\}$ is the radial number which corresponds to the number of maxima of the electric field intensity along the $\hat{r}$ axis. $p = \{0, 1 \ldots\}$ stands the polar number and $m = \{1, 2 \ldots\}$ is the azimuthal number representing the number of the electric field amplitude maxima along $\hat{\varphi}$. H_p are the Hermite polynomials of degree p which determine the lateral mode profile. The Airy function determines the radial distribution of the electric field in the resonator. E_0 is a normalization constant and E'_η is the evanescence field amplitude given by the boundary conditions according to each polarization. The abbreviations in the formula are defined as

$$f^{\eta}_m(\rho) = (\rho' + \Delta'_\eta - \rho)/u_m - \alpha_q, \tag{3a}$$

$$\theta_m = (\tilde{R}_\eta/\rho')^{3/4}\frac{1}{\sqrt{m}}, \tag{3b}$$

$$u_m = 2^{-1/3}m^{-2/3}\tilde{R}_\eta, \tag{3c}$$

where α_q is the q-root of the Airy function (i.e. $Ai(-\alpha_q) = 0$) and $\tilde{R}_\eta = R_\eta + \Delta'_\eta$ is the effective radius. The functions u_m is related to the width and position of the mode maxima along the $\hat{r}$-axis inside the resonator.

The previous considerations give an account for the spatial description of the field but do not reveal the spectral resonance positions. For this we use the dispersion relation [3, 4]:

$$\omega^{\eta}_{q,p,m}\frac{n_\eta(\omega)\tilde{R}_\eta}{c} = l - \alpha_q\left(\frac{l}{2}\right)^{1/3} + \frac{2p(\sqrt{\tilde{R}_\eta} - \sqrt{\rho'}) + \sqrt{\tilde{R}_\eta}}{2\sqrt{\rho'}} - \frac{\zeta n}{\sqrt{n^2-1}} + \frac{3\alpha_q^2}{20}\left(\frac{l}{2}\right)^{-1/3}$$
$$-\frac{\alpha_q}{12}\left(\frac{2p(\tilde{R}_\eta^{3/2} - \rho'^{3/2}) + \tilde{R}_\eta^{3/2}}{\rho'^{3/2}} \cdot \frac{2n\zeta(2\zeta^2 - 3n^2)}{(n^2-1)^{3/2}}\right)\left(\frac{l}{2}\right)^{-2/3} + \mathcal{O}(l^{-1}) \tag{4}$$

with $l = p + |m|$ and $\zeta = 1$ for TE and n^{-2} for TM modes. The first part clearly relates to the standard Fabry-Perot equation and the higher order contributions take the effects of the geometry into account. The optical FSR between modes of the same family {p,q} will remain constant for several GHz but a small dispersion contribution coming mainly from the term $\propto (l^{1/3})$ and the change in the nominal refractive index $n(\omega)$ (following the Sellmeier equation [5]).

B. Second order interaction

To derive the rate equations describing our comb, we start from the nonlinear interaction energy which is a function of the nonlinear polarization $P^{(2)} = \chi^{(2)} E^2$ and the entire electric field $E = \sum_k E_k$. In general, $\chi^{(2)}$ is a tensor, but since all fields are parallelly polarized in our experiment, the vector equation becomes scalar. The nonlinear energy can be written as [6]:

$$\langle U^{(2)} \rangle = \int dV \int dt \left\langle E \frac{\partial P^{(2)}}{\partial t} \right\rangle. \tag{5}$$

The interaction Hamiltonian can be derived from this expression using the electric field operators in the second quantization which are given as: $\hat{E}_k(\mathbf{r},t) = i\sqrt{\frac{\hbar\omega}{2\epsilon_k V_k}}(\psi_k(\mathbf{r})\hat{a}_k e^{-i\omega_k t} - \psi_k^*(\mathbf{r})\hat{a}_k^\dagger e^{i\omega_k t})$, where ψ_k is the spatial mode distribution, V_k is the effective mode volume, ϵ_k the permittivity, ω_k the angular frequency, and a_k ($a_k^\dagger$) stand for the annihilation (creation) operator, respectively.

First, let us consider only three interacting fields $E = E_1 + E_2 + E_3$. The Hamilton operator for this interaction can be obtained by rewriting Eq. (5) using the electric field operators and assuming the energy conservation condition of $\omega_3 = \omega_1 + \omega_2$ (corresponding to sum frequency generation):

$$\hat{H}_{\text{int}} = 2\epsilon_0 \chi^{(2)} \sqrt{\frac{\hbar^3 \omega_1 \omega_2 \omega_3}{8\epsilon_1\epsilon_2\epsilon_3 V_1 V_2 V_3}} \int dV (\psi_3^* \psi_2 \psi_1 \hat{a}_3^\dagger \hat{a}_2 \hat{a}_1 + \psi_3 \psi_2^* \psi_1^* \hat{a}_3 \hat{a}_2^\dagger \hat{a}_1^\dagger). \tag{6}$$

The first term inside the integral describes the creation of a photon with frequency ω_3 from the annihilation of two photons with frequencies ω_1 and ω_2. The second term represents the decay of ω_3 into ω_1 and ω_2. Both processes in the Hamiltonian set the bidirectionally of this effect. The strength of the nonlinear interaction is governed by the overlap between the modes and the nonlinearity of the material resulting in the single photon coupling rate

$$g = 2\epsilon_0 \chi^{(2)} \sqrt{\frac{\hbar \omega_1 \omega_2 \omega_3}{8\epsilon_1\epsilon_2\epsilon_3 V_1 V_2 V_3}} \int dV \psi_3^* \psi_2 \psi_1. \tag{7}$$

In the present system the three field distributions are rotationally symmetric (see Eq. (2)) and therefore the integral over the angular contribution is only nonzero if the relation $m_3 = m_1 + m_2$ is fulfilled [1].

In a closed (lossless) system with real $\chi^{(2)}$, the nonlinear coupling constant g is also real which dictates that the energy exchange between the participating fields oscillates with angular frequency g. The interaction Hamiltonian becomes

$$\hat{H}_{\text{int}} = \hbar g (\hat{a}_3^\dagger \hat{a}_2 \hat{a}_1 + \hat{a}_3 \hat{a}_2^\dagger \hat{a}_1^\dagger). \tag{8}$$

For the special case that one of the modes is a bright coherent field (classical field: $\hat{a}_1 \to \alpha$ with α being the square root of the pump photon number) and no kind of depletion of this field over the relevant time scale, the Hamiltonian becomes:

$$\hat{H}_{\text{int}} = \hbar \alpha g (\hat{a}_3^\dagger \hat{a}_2 + \hat{a}_3 \hat{a}_2^\dagger). \tag{9}$$

This is also known as the beam splitter Hamiltonian and αg can be interpreted as the photon conversion rate from mode $\hat{a}_2$ to mode $\hat{a}_3$ and vice versa. The result of this kind of linearisation of the Hamiltonian is known as the zero-photon process characterized by photons scattering from one mode into another without changing the total number of photons [7].

C. $\chi^{(2)}$-comb generation

With a strong microwave pump field the nonlinear process can cascade. In particular if multiple modes ω_k are equidistantly separated from the optical pump ω_0 and have all the same nonlinear coupling constant g, both the sum- and difference frequency generation process cascades. Phase matching limits the interaction to only neighboring modes and the Hamiltonian can be written as:

$$\hat{H}_{\text{int}} = \hbar|\alpha|g \sum_{k=-N}^{N-1} (\hat{a}_k \hat{a}_{k+1}^{\dagger} + \hat{a}_k^{\dagger} \hat{a}_{k+1}), \tag{10}$$

where $2N+1$ is the number of modes involved in the system. To describe the time evolution of this system we calculate the equations of motion of each mode's field operator using the Heisenberg picture. For a given mode k it holds:

$$\dot{\hat{a}}_k = \frac{i}{\hbar}[\hat{H}_{\text{int}}, \hat{a}_k] = -i\sqrt{n_\Omega} g(\hat{a}_{k-1} + \hat{a}_{k+1}), \tag{11}$$

where a_k denotes the k-th participating optical mode and n_Ω is the number of microwave photons in the system.

Up to now we have considered an idealized system without losses. In a real system, the optical cavity is an open system which is coupled externally by a coherent microwave tone and optical laser. Moreover, there is energy loss due to material absorption, scattering, radiation loss, etc. We introduce these two features in the last equation using the electric field internal loss rate γ' and the coupling rate γ. In addition, we also assume that the fields are classical, neglecting vacuum fluctuations effects. Then, we get the following equation in the rotating wave approximation for an optical pump at frequency ω_k' and microwave tone at Ω:

$$\dot{A}_k = -(i\delta\omega_k + \gamma + \gamma')A_k - i\sqrt{n_\Omega} g(A_{k-1}e^{i\phi_\Omega} + A_{k+1}e^{-i\phi_\Omega}) + \sqrt{2\gamma} A_{\text{in}} \delta(\omega_k - \omega_{k'}). \tag{12}$$

Where A_k denotes the slowly varying electric field amplitude of the mode k, $\delta\omega_k = \omega_k - (\omega_{k'} + (k-k') \cdot \Omega)$ is the total detuning between the sideband signal to its corresponding mode k, respectively. We have introduced the optical pump force A_{in}, which is used here to represent an optical monochromatic driving field with the amplitude given as function of the optical pump power P_0 as $|A_{\text{in}}| = \sqrt{P_0/\hbar\omega_{k'}}$. For a resonant microwave mode the microwave photon number is given by: $n_\Omega = 2\gamma_\Omega P_\Omega/\hbar\Omega(\gamma_\Omega + \gamma'_\Omega)^2$, where P_Ω stands for the input power and γ_Ω and γ'_Ω stand for the coupling and internal loss field rates, respectively.

In steady state, the time derivatives are zero and Eq. (12) becomes a simple set of linear equations:

$$\begin{pmatrix} 0 \\ 0 \\ 0 \\ \vdots \\ 0 \end{pmatrix} = - \begin{bmatrix} (1+i\Delta_0) & -i\sqrt{G}e^{-i\phi_\Omega} & i\sqrt{G}e^{+i\phi_\Omega} & 0 & \cdots & 0 \\ i\sqrt{G}e^{+i\phi_\Omega} & (1+i\Delta_{+1}) & 0 & i\sqrt{G}e^{-i\phi_\Omega} & \cdots & 0 \\ \sqrt{G}e^{-i\phi_\Omega} & 0 & \ddots & \ddots & \ddots & \vdots \\ 0 & i\sqrt{G}e^{+i\phi_\Omega} & \ddots & \ddots & \ddots & i\sqrt{G}e^{+i\phi_\Omega} \\ \vdots & \ddots & \ddots & \ddots & (1+i\Delta_{+N}) & 0 \\ 0 & 0 & \cdots & i\sqrt{G}e^{-i\phi_\Omega} & 0 & (1+i\Delta_{-N}) \end{bmatrix} \begin{pmatrix} A_0 \\ A_{+1} \\ A_{-1} \\ \vdots \\ A_{-N} \end{pmatrix} + \begin{pmatrix} \sqrt{\frac{2\gamma}{\Gamma^2}} A_{\text{in}} \\ 0 \\ 0 \\ \vdots \\ 0 \end{pmatrix}, \tag{13}$$

where we define the cooperativity $G = n_\Omega g^2/\Gamma^2$ as a dimensionless parameter, the total coupling rate $\Gamma = \gamma + \gamma'$, and the normalized detuning of the optical sidebands $\Delta_k = \delta\omega_k/\Gamma$.

This set of linear equations is numerically solvable for any arbitrary detuning, coupling strength or number of modes. Analytical solutions can be found for special cases and boundary conditions. We can calculate the total electric field, for an optical pump at ω_0, assuming a non dispersive system (fixed free spectral range, which leads to only first order contributions in Eq. (4)), a microwave tone frequency at $\Omega = \text{FSR}$, and an infinite number of modes ($N \to \infty$):

$$\sum_{-\infty}^{\infty} (1+i\Delta_k)A_k + i\sqrt{G} \sum_{-\infty}^{\infty} (A_{k-1}e^{i\phi_\Omega} + A_{k+1}e^{-i\phi_\Omega}) = \sum_{-\infty}^{\infty} \sqrt{\frac{2\gamma}{\Gamma^2}} A_{\text{in}} \delta(\omega_k - \omega_0) \tag{14}$$

We can now use the definition of the total electric field $A(t) = \sum_{-\infty}^{\infty} A_k e^{-i\Omega k t}$ and consider only constant detuning $\Delta = \Delta_k = \delta\omega/\Gamma$ and write:

$$(1+i\Delta)A(t) + i\sqrt{G}A(t)(e^{i(\Omega t + \phi_\Omega)} + e^{-i(\Omega t + \phi_\Omega)}) = \sqrt{\frac{2\gamma}{\Gamma^2}} A_{\text{in}}.$$

The solution for the total field inside the optical system is therefore:

$$A(t)=\frac{\sqrt{\frac{2\gamma}{\Gamma^2}}A^{\rm in}}{1+i\Delta+2i\sqrt{G}\cos(\Omega t+\phi_\Omega)}. \tag{15}$$

This solution for the field with respect to the time gives us information of the whole but not of a single sideband of the comb. From Eq. (12) follows that only neighboring modes interact. Intuitively this can be understood such that a given sideband acts as pump mode for the next order sideband resulting in an exponential decay of the power of the sidebands.

We profit from this feature and use the ansatz $\sim (e^{-\beta(G)})^k$ for the sidebands, where $\beta(G)$ is an arbitrary function. Moreover, we can set the condition that the comb must be symmetric around the pump. Then, we can find the Fourier coefficients A_k by using Eq. (15) as follows:

$$\begin{aligned}
A(t)=\sum_{-\infty}^{\infty}A_k(G)e^{-i\Omega kt} &= A_0(G)\left(\sum_{0}^{\infty}(-ie^{-\beta(G)})^k e^{-i\Omega kt-ik\phi_\Omega}+\sum_{-\infty}^{-1}(-ie^{-\beta(G)})^{-k}e^{i\Omega kt+ik\phi_\Omega}\right)\\
&= A_0(G)\left(\sum_{0}^{\infty}(-ie^{-\beta(G)})^k e^{-i\Omega kt-ik\phi_\Omega}+\sum_{1}^{\infty}(-ie^{-\beta(G)})^{k}e^{i\Omega kt+ik\phi_\Omega}\right)\\
&= A_0(G)\left(\sum_{0}^{\infty}(-ie^{-\beta(G)})^k e^{-i\Omega kt-ik\phi_\Omega}+\sum_{0}^{\infty}(-ie^{-\beta(G)})^{k}e^{i\Omega kt+ik\phi_\Omega}-1\right)\\
&= A_0(G)\left(\frac{1}{1+ie^{-\beta(G)-i\Omega t-i\phi_\Omega}}+\frac{1}{1+ie^{-\beta(G)+i\Omega t+i\phi_\Omega}}-1\right)\\
&= A_0(G)\left(\frac{(1+e^{-2\beta})}{1-e^{-2\beta}+2ie^{-\beta}\cos(\Omega t+\phi_\Omega)}\right)
\end{aligned} \tag{16}$$

This can be set equal to Eq. (15):

$$\begin{aligned}
A_0(G)\left(\frac{(1+e^{-2\beta})}{1-e^{-2\beta}+2ie^{-\beta}\cos(\Omega t+\phi_\Omega)}\right) &= \frac{\sqrt{\frac{\gamma}{2\Gamma^2 G}}A^{\rm in}}{\frac{1+i\Delta}{2\sqrt{G}}+i\cos(\Omega t+\phi_\Omega)}\\
A_0(G)\frac{\frac{1+e^{-2\beta}}{2e^{-\beta}}}{\frac{1-e^{-2\beta}}{2e^{-\beta}}+i\cos(\Omega t+\phi_\Omega)} &= \frac{\sqrt{\frac{\gamma}{2\Gamma^2 G}}A^{\rm in}}{\frac{1+i\Delta}{2\sqrt{G}}+i\cos(\Omega t+\phi_\Omega)}.
\end{aligned} \tag{17}$$

From the last equation we find the functional dependence of β:

$$e^{-\beta(G,\Delta)}=\frac{1+i\Delta}{2\sqrt{G}}\left(-1+\sqrt{1+4\frac{G}{(1+i\Delta)^2}}\right). \tag{18}$$

We can use this to write down the amplitude for the pump field inside the resonator:

$$A_0(G,\Delta)=\sqrt{\frac{2\gamma}{\Gamma^2}}\frac{A^{\rm in}e^{-\beta}}{\sqrt{G}+\sqrt{G}e^{-2\beta}}=\sqrt{\frac{2\gamma}{\Gamma^2}}\frac{\left(-1+\sqrt{1+4\frac{G}{(1+i\Delta)^2}}\right)\times(1+i\Delta)A^{\rm in}}{4G-(1+i\Delta)^2\times\left(-1+\sqrt{1+4\frac{G}{(1+i\Delta)^2}}\right)},. \tag{19}$$

Where the amplitudes of the sidebands decrease with their order, since $|e^{-\beta(G)}|<1$ in order for the sums above to converge. The electric field of each sideband in the cavity is given by:

$$A_k(G)e^{-i\Omega kt}=\sqrt{\frac{2\gamma}{\Gamma^2}}\frac{(-ie^{-\beta(G,\Delta)})^{|k|}e^{-i\Omega kt-ik\phi_\Omega}e^{-\beta(G,\Delta)}}{\sqrt{G}+\sqrt{G}e^{-2\beta(G,\Delta)}}A^{\rm in} \tag{20}$$

These last two equations describe quantitatively the exponential envelope for the sideband field amplitudes. Moreover, they predict that the exponential decay between neighboring sidebands decreases as G increases. This leads to the OFC becoming wider with increasing parameter G. The limit is given by the coefficient $|e^{-\beta(G)}|\to 1$ for $1/\sqrt{G}\to 0$. Moreover, it follows that in the range $4G\gg 1$, it holds: $\beta(G)=\frac{1}{2\sqrt{G}}$.

In a coupled system there are some external factors, such as mode overlap mismatch between the resonator and the coupler (prism), that play a role in the output power of the comb's sidebands. Furthermore, the condition of critical ($\gamma=\gamma'$), under- ($\gamma<\gamma'$) and over-coupling ($\gamma>\gamma'$) influences the output power [1]. Therefore, the electric

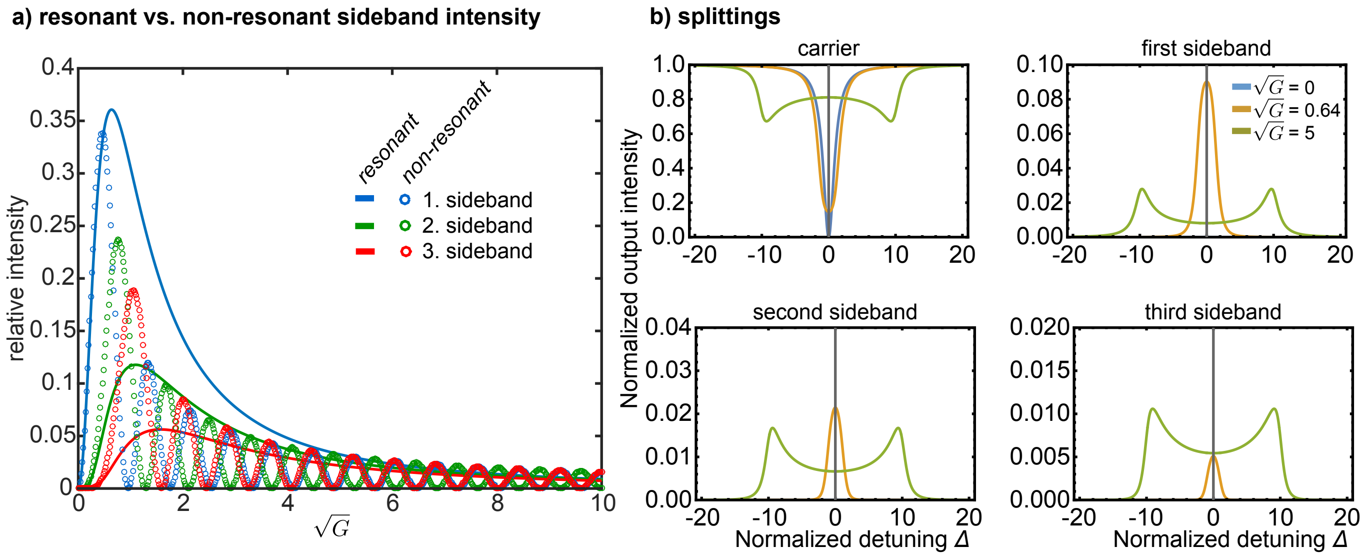

Supplementary Figure S1. Comparison between sidebands of a resonant and non-resonant system and mode a) The normalised sidebands of both system behave similar for low values of $\sqrt{G}$. As G increases the sidebands power of the non-resonant system starts to oscillate (dots) following the general trend of Bessel functions. On the contrary, the sidebands of the resonant system show a more stable behaviour (solid lines). b) Mode splitting for a critical coupled system. The carrier and the first three sidebands splittings follow $\Upsilon \approx 4\sqrt{G} - 1.2$.

field amplitude of each sideband coming out from the system and the total electric field output with a perfect mode overlap is given by:

$$A^{\text{out}}(t) = -A^{\text{in}} + \sqrt{2\gamma}A(t)$$
$$A^{\text{out}}(t) = \sum_{-\infty}^{\infty} A_k^{\text{out}}(t) = \sum_{-\infty}^{\infty}\left(-\delta_{0,k}A^{\text{in}} - \sqrt{2\gamma}A_0(G,\Delta)\times(-ie^{-\beta(G,\Delta)})^{|k|}e^{-i\Omega k t}\right)$$
$$A^{\text{out}}(t) = \frac{2\gamma/\Gamma - 1 - i(\Delta + 2\sqrt{G}\cos(\Omega t + \phi_\Omega))}{1 + i(\Delta + 2\sqrt{G}\cos(\Omega t + \phi_\Omega))}A^{\text{in}}(t). \tag{21}$$

This extended expression from Ref. [8] contains the whole information of the system such as the reflected carrier field and the sidebands' amplitude and phase. Under the condition that optic and microwave fields on are on resonance an initially strongly overcoupled configuration $\gamma/\Gamma \approx 1$, maximizes the sidebands' output amplitudes:

$$A^{\text{out}}(t) \approx \exp[-2i\arctan(2\sqrt{G}\cos(\Omega t + \phi_\Omega))]A^{\text{in}}(t). \tag{22}$$

It is worth to compare this expression with the output electric field of a non-resonant phase modulator which is given by [9]:

$$A^{\text{out}}(t) = \exp[-i\xi\cos(\Omega t)]A^{\text{in}}(t)$$
$$= A^{\text{in}}(t)\sum_{l=-\infty}^{\infty}(-i)^l J_l(\xi)e^{-il\Omega t}, \tag{23}$$

where J_l are the usual l-th order Bessel functions of first kind and ξ is the modulation index. Both expressions coincide for small values of G where the small angle approximation $\arctan(x) \approx x$ holds. From this comparison, we find the relation between the cooperativity G and the modulation index to be $\xi = 4\sqrt{G}$ and the relation between the phases of the sidebands relative to the carrier [10].

In Fig. 2 we show the dependence of frequency combs with respect to the cooperativity G, where the sidebands' power follows an exponential envelope as described in Eq. (20). Another important aspect of this systems is given by the behaviour of the sidebands' amplitude. In a non-resonant electro-optic modulator the sidebands' power oscillates as the modulation index increases. On the other hand, in a resonant system the sidebands reach a maximum given by the initial coupling configuration and then they also decreases monotonically in G. Both effects are illustrated in Fig. S1(a). In our system the maximum power of the first order sideband $|A_1^{\text{out}}|^2/|A_0^{\text{in}}|^2 = 0.36$ for $\sqrt{G} \approx 0.64$. These values depend on the number of the optical modes involved. For example, for three optical modes the first sidebands' maximal normalized power is 0.5 at $\sqrt{G} = 0.5$.

Another important feature of the multiple resonant system is given by the mode splitting of the reflected signal and the sidebands. This is analytically described by Eq. (20) and a critically coupled carrier behaves as:

$$\Upsilon \approx 4\sqrt{G} - 1.2 \text{ for } G > 1. \tag{24}$$

The mode splitting of the carrier and the sidebands follow the pattern $\Upsilon \sim 4\sqrt{G}$ which is shown analytically in Fig. S1(b) and experimentally in Fig. 2b. The splitting in terms of absolute frequency is given by $4\sqrt{n_\Omega}g$, which is a factor two larger than in the case of two optical modes coupled with $\sqrt{n_\Omega}g$ (e.g. in the case for optomechanics or single sideband modulation) and a factor $\sqrt{2}$ larger than in the case of two symmetric sidebands, given as $\sqrt{2}\sqrt{n_\Omega}g$. The splitting reflects how strong the interaction between the modes are and the effective coupling strength of such a multimode system can be extracted from the eigenvalues of the dynamic matrix in Eq. (13). For $N \to \infty$ the matrix has infinite eigenvalues and corresponding eigenvectors. Under the constraint of a fixed FSR $= \Omega$ and driving only the central mode A_0, we choose the eigenvalue for the eigenvector with the highest $|A_0|$, which is given by: $\eta_\pm = \pm i\sqrt{4n_\Omega}g - 2\Gamma$. This leads to the splitting $|\eta_+ - \eta_-| = 4\sqrt{n_\Omega}g$. The factor 1.2 in Eq. (24) changes slightly according to the sideband order and initial coupling conditions. The splitting broadens the optical modes which then allows the comb to spread up to the sideband order whose dispersion induces a detuning $\delta\omega_k$ which equals to $(2\sqrt{G} - 0.6)\Gamma$ as shown in Fig. 2a.

Another important feature intrinsically connected to the splitting is the generation of pulses. If the carrier is initially resonant and the system is critically coupled, then the reflection is ideally zero. The term $2\sqrt{G}\cos(\Omega t)$ in the denominator in Eq. (15) acts like an effective shift of the optical resonance which oscillates with frequency $\Omega/2\pi$ and amplitude $2\sqrt{G}$. This will amplitude modulate the reflected signal with two well defined dips during a period of time $2\pi/\Omega$. The duration of the generated pulses $\Delta\tau$ is $\approx \frac{1}{\Omega\sqrt{G}}$ for the case of $4G \gg 1$.

From Eq. (20) we extract information about the noise (phase or intensity) in any electrooptical modulator, which depends linearly on the sideband order. In case of the microwave phase noise $\phi_\Omega(t)$, which we assume to vary around an initial phase offset ϕ_Ω with $\phi_\Omega(t) = \phi_\Omega + \Delta\phi_\Omega(t)$. The phase noise of the sideband k becomes then $\sim k\Delta\phi_\Omega(t)$. This linear noise amplification of the microwave noise can be use to characterize microwave sources. On the oder hand, optical phase or intensity noise of the source is the same for each sideband order.

D. Efficiency and π-Voltage

The efficiency of an electro-optic modulator can be given in terms of V_π. This is the required voltage applied to an electro-optic phase modulator to shift the phase of the optical carrier by π. We can extract this information from the nonlinear coupling constant g which can be defined as the phase shift induced to the optical carrier by a single microwave photon per roundtrip time [11]:

$$\frac{\Delta\phi}{\tau} = g. \tag{25}$$

Moreover, the classical microwave field amplitude α in case of a resonant microwave system is given in terms of the input power P_{AC} as:

$$n_\Omega = |\alpha|^2 = \frac{2\gamma_\Omega P_{\mathrm{AC}}}{\hbar\Omega((\gamma_\Omega + \gamma'_\Omega)^2 + \Delta\Omega^2)}, \tag{26}$$

where n_Ω is the mean photon number in the mode, $\Delta\Omega$ the pump detuning, γ_Ω and γ'_Ω are the corresponding coupling and loss rates of mode fields. The standard relation between power and a sinusoidal peak voltage V_p in an AC circuit holds:

$$P_{\mathrm{AC}} = \mathrm{Re}\left(\frac{V_p^2}{2Z}\right), \tag{27}$$

where Z is the load impedance which in most cases is 50 Ohm. In the optical resonator the carrier stays an average time τ_p before it is outcoupled or absorbed. We find the voltage V_π by rewriting the relation $\alpha g \tau_p = \pi$ in terms of the voltage and it follows:

$$V_\pi = \frac{\pi}{g\tau_p}\sqrt{\frac{Z\hbar\omega_\Omega(\gamma_\Omega + \gamma'_\alpha)^2}{\gamma_\Omega}}. \tag{28}$$

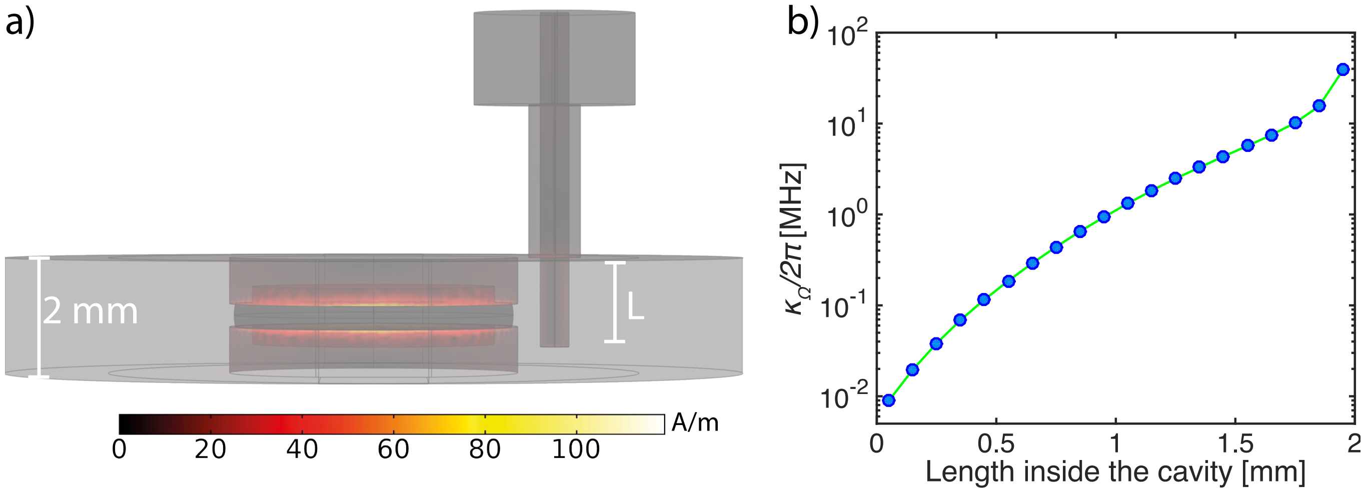

Supplementary Figure S2. a) Surface current distribution inside the 3D cavity and the coaxial probe. The length L is change from 0.05 to 1.95 mm and the excitation port power was set to 1 mW. b) Exponential behaviour of the coupling strength κ_Ω.

For our experimental parameters, we estimate the π-voltage to be $V_\pi \approx 260$ mV. The ratio of the power consumption between a normal and resonant modulation is given by the ratio squared of their corresponding V_π. In our case this means that the power consumed is 100 times less than the best modulator so far reported at this frequencies. Obviously this enhancement limits the bandwidth, but in our application as a frequency comb source this does not pose a problem.

E. Microwave Coupling

We decided to use a coaxial probe coupler because it allows us to engineer a compact design for the cavity and offers an easy control over the coupling strength without modifying the rest of the cavity's geometry. The usual coupling probe is made by stripping the transmission line coaxial cable and putting the core inside the cavity leaving the outer braided shield in contact with the metal cavity. The length of the probe is ideally set to a quarter of the wavelength such that the input impedance is nearly equivalent to that of an open circuit. The voltage difference between the probe and the adjacent metal wall of the resonator generates an electric field between them and there is also a small current flowing through the probe. The coupler's field radiates the energy similar to a monopole antenna and the electric field lines are perpendicular to the probe surface and the 3D inner surface. The pin coupler excites only modes with the electric field parallel to its own field lines and the coupling strength depends on the mode overlap of the coupler's and the cavity's modes. In this way we can choose to which mode we want to couple by locating the probe near to its maximum electric field amplitude (strong coupling) or its minimum (no coupling). We have used only one port for this experiment and we characterize the system always in reflection. A second port would enable us to also measure transmission. However, we want the photons to stay in the cavity as long as possible and once a photon is inside the cavity, a second coupling port would add another loss channel, thereby reducing the effective microwave photon lifetime.

Experimentally, a SMA connector can be fixed to the cavity's outer surface. The pin attached to it extends into the microwave cavity through a feedthrough with radius r_h, we choose r_h such as: $0.36 = \log_{10}(r_h/r_p)$ resulting in an impedance of 50 Ohm. From the COMSOL eigenfrequency simulations we known the mode's distribution and we can place the pin close to the mode maxima to assure good mode overlap and its length can be optimized to achieve critical coupling.

We ran the transient COMSOL simulations as depicted in Fig. S2, where we have simulated the pin's head, the feedthrough and the cavity. The pin's head is set as coaxial port and excited over the frequencies around the resonance given by the eigenfrequency simulation. The simulated coupling rate of the intensity $\kappa_\Omega = 2\gamma_\Omega$ as a function of the pin's length is shown in a logarithmic plot in Fig. S2b. The exponential growth of κ_Ω makes it a very sensitive parameter not only to the pin's length but also to possible bends. In our design, which has a strong electric field confinement, it requires therefore that the probe gets closer to the rings which increases the current flowing on the pin. Therefore, the pin itself contributes to ohmic losses in the system. The presence of the pin modifies also the cavity mode distribution changing the resonance frequency by several MHz.

[1] D. V. Strekalov, C. Marquardt, A. B. Matsko, H. G. L. Schwefel, and G. Leuchs, "Nonlinear and quantum optics with whispering gallery resonators," Journal of Optics, vol. 18, no. 12, p. 123002, 2016.
[2] I. Breunig, B. Sturman, F. Sedlmeir, H. G. L. Schwefel, and K. Buse, "Whispering gallery modes at the rim of an axisymmetric optical resonator: Analytical versus numerical description and comparison with experiment," Opt. Express, vol. 21, pp. 30683–30692, Dec 2013.
[3] M. R. Foreman, F. Sedlmeir, H. G. L. Schwefel, and G. Leuchs, "Dielectric tuning and coupling of whispering gallery modes using an anisotropic prism," J. Opt. Soc. Am. B, vol. 33, pp. 2177–2195, Nov 2016.
[4] Y. A. Demchenko and M. L. Gorodetsky, "Analytical estimates of eigenfrequencies, dispersion, and field distribution in whispering gallery resonators," J. Opt. Soc. Am. B, vol. 30, pp. 3056–3063, Nov 2013.
[5] D. E. Zelmon, D. L. Small, and D. Jundt, "Infrared corrected Sellmeier coefficients for congruently grown lithium niobate and 5 mol. % magnesium oxide–doped lithium niobate," J. Opt. Soc. Am. B, vol. 14, pp. 3319–3322, Dec. 1997.
[6] Y. R. Shen, "Permutation symmetry of nonlinear susceptibilities and energy relation," Phys. Rev., vol. 167, pp. 818–821, Mar 1968.
[7] C. K. Law, "Effective hamiltonian for the radiation in a cavity with a moving mirror and a time-varying dielectric medium," Phys. Rev. A, vol. 49, pp. 433–437, Jan 1994.
[8] V. S. Ilchenko, A. A. Savchenkov, A. B. Matsko, and L. Maleki, "Whispering-gallery-mode electro-optic modulator and photonic microwave receiver," J. Opt. Soc. Am. B, vol. 20, pp. 333–342, Feb. 2003.
[9] D. M. Pozar, Microwave Engineering. Hoboken, NJ: Wiley, 4 edition ed., Nov. 2011.
[10] P. Hobbs, Building Electro-Optical Systems: Making It all Work. Wiley Series in Pure and Applied Optics, Wiley, 2011.
[11] M. Tsang, "Cavity quantum electro-optics," Physical Review A, vol. 81, p. 063837, June 2010.